

Sodium butyrate ameliorates fluorosis-induced neurotoxicity by regulating hippocampal glycolysis in vivo

Yangjie Li

Shenyang Medical College

Zhengdong Wang

Shenyang Medical College

Jing Li

Shenyang Medical College

Yang Yu

Shenyang Medical College

Yuan Wang

Central Hospital Affiliated to Shenyang Medical College

Xiaoxia Jin

Shenyang Medical College

Yun Dong

Central Hospital Affiliated to Shenyang Medical College

Qingsong Liu

Shenyang Medical College

Xiaoxu Duan

Shenyang Medical College

Nan Yan (✉ yannan369@163.com)

Shenyang Medical College

Research Article

Keywords: fluorosis, sodium butyrate, glycolysis, nervous system, PI3K/AKT/HIF-1 α

Posted Date: November 2nd, 2022

DOI: <https://doi.org/10.21203/rs.3.rs-2222214/v1>

License:   This work is licensed under a Creative Commons Attribution 4.0 International License.

[Read Full License](#)

Additional Declarations: No competing interests reported.

Version of Record: A version of this preprint was published at Biological Trace Element Research on January 30th, 2023. See the published version at <https://doi.org/10.1007/s12011-023-03583-6>.

Abstract

Fluorosis can induce neurotoxicity. Sodium butyrate (SB), a histone deacetylase inhibitor, has important research potential in correcting glucose metabolism disorders and is widely used in a variety of neurological diseases and metabolic diseases, but it is not yet known whether it plays a role in combating fluoride-induced neurotoxicity. This study aims to evaluate the effect of SB on fluoride neurotoxicity and the possible associated mechanisms. The results of HE staining and Morris water maze showed that in mice exposed to 100 mg/L fluoride for three months, the hippocampal cells arranged in loosely with large cell gaps and diminished in number. In addition, 1000 mg/kg/day SB treatment improved fluoride-induced neuronal cell damage and spatial learning memory impairment. Western blotting showed that the abundance of malate dehydrogenase 2 (MDH2) and pyruvate dehydrogenase (PDH) in the hippocampus of mice increased after fluorosis, while the abundance of pyruvate kinase M (PKM), lactate dehydrogenase (LDH) and hexokinase (HK) decreased. SB treatment reversed the decreased glycolysis in the hippocampus of fluorosis mice. We suspected that the PI3K/AKT/HIF-1 α pathway may be involved in mediating the protective effects of SB against fluorosis invasion in the hippocampus. These results suggested that SB could ameliorate fluorosis-induced neurotoxicity, which might be linked with its function in regulating glycolysis as well as inhibition of the PI3K/AKT/HIF-1 α pathway.

1. Introduction

Fluoride is one of the essential trace elements for human health and is found throughout the environment, for example, in soil, air, and tap water[1]. Although fluoride has been used around the world to prevent and control dental caries, long-term excessive fluoride intake can cause damage to many systems in the body[2, 3]. Nowadays, the toxic side effects of fluoride on the brain have become a topic of research focus in environmental toxicology[4]. High dosage of fluoride can penetrate many areas of the brain, such as the hippocampus, cerebellum, and cortex, by crossing the blood-brain barrier[5], eventually leading to drowsiness, insomnia, headache, dizziness, and deterioration in learning and memory capacity[6]. Currently, the possible mechanisms underlying such effects involve cholinergic pathways, oxidative stress, hippocampal calcium signaling, and synaptic plasticity[7, 8, 9].

In recent years, several studies have found that decreased glucose utilization occurs in a variety of neurological diseases. Improving the status of brain glucose metabolism has become an emerging strategy in the treatment of many chronic nervous system diseases such as Alzheimer's disease, stroke, and depression[10, 11, 12]. As one of the major pathways of glucose metabolism, abnormal glycolysis is considered to be an initiating or promoting factor in many neurological diseases[13]. Compared with those in normal mice, the protein expression and transcription levels of the glycolysis enzymes lactate dehydrogenase A (LDHA), pyruvate kinase M (PKM), and hexokinase 2 (HK) are inhibited in Alzheimer's disease mice, and the contents of lactate and NAD⁺ are decreased. However, measurement of cell oxygen consumption rates indicated the activation of mitochondrial OXPHOS levels when glycolysis inflow was insufficient and energy supply was low. Promoting glycolysis and reducing OXPHOS activation can thus improve the role of astrocytes in supporting neuronal activity and function[14].

In addition to the glycolysis catalyzed by LDH, pyruvate (an intermediate of glucose metabolism) is also metabolized by OXPHOS[15]. Recent studies have shown that pyruvate dehydrogenase A1 (PDHA1), dihydrolipoamide acetyltransferase (DLAT), and dihydrolipoamide dehydrogenase (DLD), which encode either subunit E1, E2, or E3 of the pyruvate dehydrogenase (PDH) complex respectively, are promoted to different degrees in traumatic brain injury[16]. Isocitrate dehydrogenase (IDH), succinate dehydrogenase (SDH), and malate dehydrogenase 2 (MDH2) enzymes related to the tricarboxylic acid cycle showed a similar increasing trend with the extension of injury time[17]. Glycolysis preconditioning of astrocytes attenuates trauma-induced neurodegeneration and shifts brain metabolic patterns from neuron-dominated mitochondrial respiration to astrocyte-mediated glycolysis[18].

Increasing evidence has shown that sodium butyrate (SB) can enhance neuronal activity by promoting the transport of lactic acid, a glycolytic product of astrocytes, and further maintains the energy metabolism homeostasis of the central nervous system, ultimately reducing cognitive decline in Alzheimer's disease mice[19, 20]. Butyric acid, the active ingredient of SB, belongs to the short-chain fatty acids (SCFAs), which are produced by intestinal flora fermenting dietary fiber[21]. Butyric acid is an endogenous substance in the human body and therefore has little toxicity[22]. According to the gut–brain axis hypothesis, SCFAs can achieve bidirectional communication between the brain and the gut by regulating intestinal homeostasis and neuroimmunology[23]. In addition, SB is one of the most commonly used histone deacetylase inhibitors and has been shown to have neuroprotective effects in various neurological disease models, such as of Alzheimer's disease, ischemic stroke, and neonatal hypoxic encephalopathy[24, 25, 26]. However, whether SB can protect the hippocampus from fluoride-induced neurotoxicity and imbalanced metabolism, and the possible mechanism of its potential protective effect, has not been studied in depth.

The PI3K/AKT signaling pathway is involved in the maintenance of central nervous system homeostasis[27]. In addition, PI3K/AKT/HIF-1 α may be involved in the transformation of cell metabolism. The activation of PI3K/AKT/HIF-1 α can directly promote the transition in cancer cell metabolism from OXPHOS to aerobic glycolysis[28, 29]. In addition, the mechanism involves alterations in the PI3K/AKT/HIF-1 α signaling pathway, and the addition of the PI3K inhibitor LY294002 leads again to inhibition glycolysis, which had been restored after treatment with antagonists[30]. Therefore, we speculate that the neuroprotective effect of SB is related to PI3K/AKT/HIF-1 α .

In this study, HE staining and Morris water maze confirmed that long-term excessive fluoride exposure induced hippocampal damage and spatial learning and memory impairment in mice. The results of Western blot and biochemical tests showed that glycolysis was inhibited in the hippocampi of fluorosis mice and SB could ameliorate fluorosis-induced neurotoxicity, which might be linked with its function in regulating glycolysis and pyruvate metabolism as well as inhibition of the PI3K/AKT/HIF-1 α pathway.

2. Materials And Methods

2.1. Animals and Treatment

A total of 50 newly weaned ICR male mice were purchased from Liaoning Changsheng Biotechnology Co., Ltd (Shenyang, China), and bred at the Animal Experiment Center of Shenyang Medical College. All animals were fed standard food in the laboratory, and the laboratory temperature was set to 21–24°C, the humidity to 50 ± 5%, and the light and dark cycle to 12 h. After one week of adaptation, the mice were randomly divided into five groups: a control group (C), fluorosis group (F), sodium butyrate group (S), fluorosis and 500 mg/kg sodium butyrate treatment group (F + S1), and fluorosis and 1000 mg/kg sodium butyrate treatment group (F + S2), with 10 mice in each group. According to the previous literature, 100mg/L sodium fluoride can cause brain damage in mice [9, 31, 32]. Except for groups C and S, all groups were provided with distilled water containing 100 mg/L fluoride (Sigma-Aldrich, St. Louis, MO, USA). Three months after exposure, mice in groups S, F + S1, and F + S2 were treated by intragastric administration of sodium butyrate (Macklin, Beijing, China) at 500 or 1000 mg/kg/day for eight weeks. Groups C and S were treated by intragastric administration of normal saline. After five months, mice were subjected to a water maze experiment, and then the hippocampi of each group were removed, washed with normal saline, and preserved at – 80°C for subsequent analysis.

All animal procedures were approved by the Experimental Animal Ethics Committee of Shenyang Medical College (SYYXY2021031502) and implemented in accordance with the Provisions on the Management of Experimental Animals in Liaoning Province.

2.2 Fluoride Ion Selective Electrode

Fluoride concentrations in urine and blood were measured according to the People's Republic of China Health Industry Standard (WS/T 89-2015 and WS/T 212–2001)[33, 34]. The mice were placed in a metabolic cage and deprived of water for 24 hours to collect urine. Subsequently, the mice were sacrificed by cervical dislocation and blood was collected from the orbit. Blood samples were centrifuged (3000rpm, 10min) for serum. Calibrate the ionometer (Leici Instrument, Shanghai, China) with standard solutions of different concentrations of fluoride. The sample and total ion concentration buffer (Leici Instrument, Shanghai, China) were added at a rate of 1:1 and placed under a fluoride ion meter for 30 seconds to measure the mean concentration.

2.3. Morris water maze

Mice were subjected to a Morris water maze (Taimeng, Sichuan, China) test for six days. The maze consists of a circular pool, escape platform, and recording equipment. The pool was divided into four quadrants, and the water was stained with edible white pigment. The walls of the quadrants were marked with different shapes to facilitate positioning, and the escape platform was hidden 2 cm under the water. The experiment consisted of five days of directional navigation and one day of spatial exploration. During the directional navigation experiment, the time it took the mice to find the platform was recorded as the escape latency period every day. If the mice could not find an escape platform within 120 s, the researchers guided them to it and left them there for 15 s. During the spatial exploration experiment, the platform was removed, and the researchers recorded the percentage of time the mice spent in the

platform's quadrant and how many times they crossed the platform. The automatic monitoring system recorded the swimming time and movement path of the mice.

2.4. HE Staining

The brain tissue was repaired and rinsed with water for 4 h. Alcohol gradient dehydration was performed, and the dissolved paraffin was infiltrated into the tissue blocks, which became hard wax blocks after cooling. The wax blocks were placed on a slicer (Leica, Heidelberg, Germany), cut into 5 μm slices, and transferred to slides. The wax blocks were placed in a temperature box at 60°C for 2 h and dried. After paraffin sections were dehydrated, hematoxylin (Solarbio, Beijing, China) was added and soaked in for 5 min. Then, the sections were rinsed with distilled water, soaked in eosin (Solarbio, Beijing, China) for 3 minutes, and sealed with neutral gum. The pathological changes in mice hippocampi were assessed by microscopy (Olympus, Tokyo, Japan).

2.5. Western blotting

After the mice were sacrificed, the hippocampus and cortex were separated, and the hippocampus was subsequently used for Western blotting. The total protein concentration was measured using a BCA protein quantitation kit (Dingguochangsheng Biotechnology, Senyang, China). The proteins were separated by sodium dodecyl sulfate–polyacrylamide gel electrophoresis (Dingguochangsheng Biotechnology) and transferred to PVDF membranes (Millipore, Billerica, MA, USA) by Trans-Blot Turbo (Hercules, CA, USA) at a constant voltage of 100 V for 1 h. The TBST diluted primary antibodies were: LDH (1:500, Wanleibio, Shenyang, China), PDH (1:1000, CST, MA, USA), MDH (1:1000, CST, MA, USA), HK (1:1000, CST, MA, USA), PKM (1:1000, Wanleibio), β -actin (1:5000, Abclone, Wuhan, China), GAPDH (1:5000, Abclone), HIF-1 α (1:1000, Abclone), PI3K (1:500, Wanleibio), AKT (1:500, Wanleibio), and P-AKT (1:500, Wanleibio). The membrane was incubated with primary antibody at 4°C for 12 h, then incubated with secondary antibody goat anti-rabbit IgG and HRP (1:6000, Wuhan, Abclone). ImageJ 1.4 (Bethesda, Maryland, USA) was used to analyze the signal strength.

2.6. Test kits

2.6.1. Lactate dehydrogenase

The LDH activity per gram of protein in mice hippocampal tissue was measured according to the LDH activity test kit (Wanleibio, Shenyang, China). Assay principle: LDH catalyzes the generation of pyruvate from lactate. Pyruvate reacts with 2,4-dinitrophenylhydrazine to form pyruvate 2,4-dinitrophenylhydrazone, which is brownish red, in an alkaline solution, and the enzyme activity can be determined according to a colorimetric enzyme standard. We added the following to a 96-well plate, in the indicated order: 20 μL of 0.01% mouse brain tissue homogenate, 25 μL of 2,4-dinitrophenylhydrazine, and 250 μL of 0.4 mol/L NaOH solution, and incubated the mixture at 37°C for 30 min. The absorbance value at 450 nm was detected using a microplate reader (Bio-Rad), and LDH activity was calculated according to the formula of the test kit. The LDH activity in tissues is expressed as U/gprot.

2.6.2. Pyruvate kinase

The PK activity of tissue protein per gram of mice hippocampus was detected using a PK activity assay kit (Jiancheng Biological Institute, Nanjing, China). Detection principle: PK catalyzes phosphoenolpyruvate and ADP to generate ATP and pyruvate. Lactate dehydrogenase further catalyzes NADH and pyruvate to produce lactic acid and NAD⁺. The NADH decline rate can reflect PK activity. To a 96-well plate, we sequentially added 5% tissue homogenate, 20 mM Tris-HCl (pH 7.5), 150 mM KCl, 5 mM MgCl₂, 0.25 mM NADH, 5 U/mL LDH, 2 mM ADP, and 1 mM phosphoenolpyruvate followed by incubation of the mixture at 37°C for 30 min. The absorbance value at 340 nm was detected using a microplate reader, and the PK activity was calculated according to the formula in the instructions. The PK activity in tissues is expressed as U/mgprot.

2.6.3. Hexokinase

The HK activity per gram of tissue protein in the hippocampus of mice was detected using the HK activity test kit (Jiancheng Biological Institute). Detection principle: HK catalyzes glucose to produce glucose-6-phosphate, and glucose-6-phosphate dehydrogenase further catalyzes glucose-6-phosphate to produce NADPH. The NADPH decline rate reflects HK activity. We added 10ul of 5% tissue homogenate, 180ul of Reagent II, 10 ul of Reagent II to 96-well plates and incubated the mixture at 37°C for 5 min. The absorbance value at 340 nm before and after incubation was detected separately by a microplate reader, and the activity of HK was calculated according to the instructions. The HK activity in tissues is expressed as U/gprot.

2.6.4. Lactate content

The lactate remaining in the mice hippocampus was determined, per gram of protein, using a lactate content test kit (Jiancheng Biological Institute). Detection principle: lactate in the role of lactate dehydrogenase produces pyruvate, while reducing NAD⁺ to NADH and H⁺. The PMSH² generated by the transfer of H⁺ to PMS can generate purple substances by reducing MTT. The absorbance of the colored substance is linearly related to the lactic acid content at 530 nm; 8% tissue homogenate and a color reagent were added to a 96-well plate in turn. After mixing, the 96-well plates were incubated in a 37°C incubator for 30 min. The absorbance value at 530 nm was detected by a microplate reader, and the lactate content was calculated according to the formula in the instructions. The lactate content in tissues is expressed as mmol/mg protein.

2.7. Statistical analysis

GraphPad Prism 8 (San Diego, CA, USA) was used for statistical analysis. All the data were expressed as the mean ± SEM. One-way ANOVA was used for comparison among multiple groups, and two-way ANOVA was used for escape latency in the Morris water maze. *P* < 0.05 was considered to indicate statistically significant differences.

3. Results

3.1. General

All mice survived during the experiment. After five months of feeding, mice in the control group and sodium butyrate group had smooth fur, good appetite and yellowish teeth. The mice treated with fluoride had reduced appetite, body and brain weight. The mice in the fluorosis group had chalky white teeth and lost their luster, and some of them had curled bodies and missing teeth. In addition, we measured the fluoride content in the blood and urine of mice. The results showed that compared with the control group, the fluoride content in blood and urine of fluoride-treated mice increased significantly, and high concentration of sodium butyrate treatment could reduce this difference ($P < 0.01$) (Table.1).

3.2. Sodium butyrate improves spatial learning and memory in fluorosis-treated mice

Morris water maze was performed after seven weeks of sodium butyrate treatment. The results showed that, compared with the control group, the latency of escape was significantly increased in the fluorosis and sodium butyrate treatment groups ($P < 0.01$); after sodium butyrate treatment, the ability of mice to find the platform was improved ($P < 0.05$) (Fig. 1a). In the space exploration experiment, the percentage of swimming time in the target quadrant and the times of crossing the escape platform in fluorosis group were reduced, to some extent, by pretreatment with 1000 mg/kg sodium butyrate ($P < 0.05$) (Fig. 1c,d). In addition, there was no significant difference in the swimming speed of mice in each group, indicating that there was no difference in the athletic ability of the mice (Fig. 1b). In conclusion, sodium butyrate had no effect on the learning and memory ability of normal mice, while the spatial learning ability and memory of mice in the fluorosis group were impaired. After sodium butyrate treatment, the spatial learning ability and memory of the mice were restored to a certain extent. The typical swimming trajectories of the mice in each group are shown in Fig. 1e.

3.3. Sodium butyrate ameliorates nervous system damage in fluorosis-treated mice

The HE staining results show that the neuronal cells in the DG, CA1, and CA3 regions of the hippocampi of the control and sodium butyrate-treated mice were normal in morphology, closely arranged, and hierarchical. In the fluorosis group, a small number of neuronal cells in the CA3 area of the hippocampus were solidly stained. The hippocampal cells in CA1 area arranged in loosely with large cell gaps and the number of hippocampal cells in DG area was reduced. In the low-and high-dose sodium butyrate-treated fluorosis mice, the degree of atrophy of neuronal cells in the CA3 area was reduced, the cell gaps in the CA1 area were basically similar to that of the control group, cell stratification was clear, and the number of neuronal cells in the DG area increased. (Fig. 2).

3.4. Sodium butyrate promotes hippocampal glycolysis in fluorosis-treated mice

The glycolysis rate is regulated by the activity and abundance of glycolysis enzymes. HK, PKM and LDH are the key enzymes to control the rate of glycolysis. We verified the protein expression and activity of HK, PKM and LDH by immunoblotting and activity assay kit. The results showed that LDH, PKM, and HK

protein expressions were decreased (Fig. 3); PK, HK, and LDH activities were inhibited in the hippocampus of fluorosis mice compared with the control group (Fig. 4A-C). At the same time, the content of glycolysis product lactate was also reduced in the hippocampus of fluorosis mice (Fig. 4D). This trend was reversed in the fluorosis and sodium butyrate-treated mice compared with the fluorosis group, where the glycolysis-promoting function was more pronounced in the high-dose antagonist group ($P < 0.05$).

3.5. Sodium butyrate inhibits hippocampal pyruvate metabolism in fluorosis-treated mice

Under the condition of sufficient oxygen supply, the intermediate product of glucose metabolism, pyruvate, can be decomposed into ATP through two pathways. One is glycolysis catalyzed by LDH, and the other is oxidative phosphorylation catalyzed by PDH. It is well known that there is some competitive inhibition of glycolysis and oxidative phosphorylation, which are the two major metabolic modes of cells. We examined the protein expression of two negative regulators of glycolysis, PDH and MDH, and the results showed that 1000 mg/kg sodium butyrate treatment promoted the inhibited PDH and MDH in the hippocampal tissues of fluorosis mice ($P < 0.05$) (Fig. 5).

3.6. Sodium butyrate promotes inhibited PI3K/AKT/HIF-1 α in fluorosis -treated mice

In addition, PI3K/AKT/HIF-1 α signaling pathway is involved in the regulation of glycolysis in cells, HIF-1 α is a key upstream regulator of glycolysis. LDH, HK, PDH and other metabolic enzymes are HIF-1 α target genes. we also detected components of the glycolysis-related pathway PI3K/AKT/HIF-1 α . The data show that the protein expressions of PI3K, AKT, P-AKT, and HIF-1 α in the fluorosis group decreased; 500 and 1000 mg/kg sodium butyrate treatment could activate PI3K/AKT/HIF-1 α signaling pathway and ultimately induce increased glycolysis in the hippocampi of fluorosis mice ($P < 0.05$) (Fig. 6).

4. Discussion

Fluoride is a trace element found widely in the natural environment[35]. Long-term excessive fluoride intake can lead to central nervous system disorders, induce neuronal apoptosis, impair hippocampal dentate gyrus neurogenesis, and eventually lead to ataxia, a decline in learning and memory, cognitive impairment, and other forms of central nervous system damage[36, 37, 38]. SB is one of numerous histone deacetylase inhibitors, and its extensive neuroprotective effect and synaptic remodeling function have great research potential[39, 40]. The present study investigated the protective role of Sodium butyrate (SB) in counteracting the effects of fluoride toxicity on the nervous system.

Firstly, we characterized the protective effect of SB on fluoride-induced neurotoxicity based on the Morris water maze test and HE staining. Fluoride markedly increased the latency of escape and decreased the time of crossing the escape platform and swimming time in mice. HE staining also showed that significant atrophy and a decreased number of nerve cells in the hippocampal CA3, CA1 and DG regions of fluorosis mice, which is consistent with previous reports[8, 41, 42]. Fernando et al. found that SB can

restore cognitive dysfunction by reducing the level of amyloid- β in the brain of Alzheimer's disease mice[43]. We also found that SB could antagonize fluoride-induced neurological behavioral and pathological injuries.

In recent years, with the deepening of research on the microbial-gut-brain axis, SB has been shown to correct disordered glucose metabolism in cells and has obvious therapeutic potential in metabolic diseases[44, 45, 46]. The main metabolic modes of glucose include glycolysis and oxidative phosphorylation (OXPHOS). Glucose is decomposed into pyruvate step by step under the catalysis of HK, PKM, PFK and other enzymes[47]. Pyruvate, which could undergo glycolysis and be converted to lactate under the catalysis of LDH, plays an important role in memory via the astrocyte-neuron lactate shuttle (ANLS)[48, 49]. It has been reported that glycolysis is inhibited in the hippocampus of Alzheimer's disease mice, and glycolytic-related enzymes and products such as PKM, HK, LDH, and lactic acid show a downward trend[14]. Pyruvate can also undergo OXPHOS under the catalysis of PDH and MDH and produce a large amount of ATP through the tricarboxylic acid cycle for efficient energy supply[50]. Glycolysis has certain competitive inhibition with OXPHOS. PDH, a negative regulator of glycolysis, is strengthened in Alzheimer's disease, Parkinson's disease, and other neurodegenerative diseases, whereas high levels of OXPHOS can promote excessive oxidative stress, increase ROS generation, and further aggravate cell damage[51, 52]. In addition, PDH and MDH act as keepers and terminators of the mitochondrial tricarboxylic acid cycle, respectively. The E1, E2, and E3 subunits (E1 (PDH), E2 (DLAT), and E3 (DLD)) of PDH and MDH are confirmed to be enhanced in traumatic brain injury[17]. Our results showed that the activity and abundance of HK, PKM and LDH were inhibited in the hippocampus of fluorosis mice, while the expression of PDH and MDH was enhanced. SB can improve nervous system injury by promoting inhibited glycolysis in fluorosis mice.

How does SB play its role in promoting glycolysis? Recent studies have found that when PI3K/AKT/HIF-1 α is over-activated, the metabolic pattern of cancer cells shifts from OXPHOS to aerobic glycolysis, a signaling pathway that is critical in regulating cell metabolism[53, 54]. Under PI3K/AKT activation, the expression of FOXO (an inhibitor of PDK) could be repressed, activating HIF-1 α to promote glycolysis[14]. HIF-1 α is a key upstream regulator of glycolysis. Ldh-a and PDK1 are the direct targets of HIF-1 α [55, 56]. HIF-1 α is involved in regulating the expression of LDH, PKM, PDK, HK, and other glycolysis-related genes. HIF-1 α overexpression can induce PDK1 phosphorylation to inactivate PDH, inhibit pyruvate entry into mitochondria, and promote glycolysis of K562 cells against 1,4-benzoquinone-induced toxicity[57]. In middle cerebral artery occlusion (MCAO) rats, treatment with SB can play a neuroprotective role by promoting the expression of PI3K and P-AKT, reducing the infarct volume after occlusion[58]. In our study, the activation of PI3K/AKT and HIF-1 α by SB notably attenuated fluoride downregulation of glycolysis, indicating that the administration of SB promotes glycolysis via the PI3K/AKT and HIF-1 α signaling pathways.

In conclusion, our data provide evidence confirming the protective effects of SB, which attenuates fluoride-induced neurotoxicity in vivo. In addition, SB could regulate glycolysis as well as PI3K/AKT/HIF-

1a. Our data, therefore, suggest that SB represents a novel therapeutic candidate for populations at high risk of fluorine poisoning.

5. Conclusions

Our study confirmed that high fluoride exposure in mice can inhibit hippocampal glycolysis and decrease brain lactic acid content, leading to nervous system damage and spatial learning and memory impairment. SB can exert neuroprotective effects by promoting inhibited glycolysis. Provide new ideas for the study of mechanisms of fluoride neurotoxicity. In addition, based on previous literature studies, PI3K / AKT / HIF-1 α signaling pathway can regulate cell glycolysis metabolism. This study observed that SB treatment promoted the inhibited PI3K / AKT / HIF-1 α signaling pathway in the hippocampus of fluorosis mice, which also created a direction for further research.

Declarations

Acknowledgments: This work was supported by grants from the National Natural Science Foundation of China (NSFC) (no. 81803200 and no. 81803180), Liaoning Province Key Research and Development Program Guidance Plan (no. 2019JH8/10300047), Shenyang Science and Technology Plan Project (no. 21-108-9-11), Shenyang Middle Younger Scientific and Technological Innovation Support Plan (no. RC200238), Project of Education Department of Liaoning Province (no. SYYX202008), Youth Foundation of Liaoning Education Department (no. LJKQZ2021173), Science and Technology Innovation Fund for Postgraduates of Shenyang Medical College (no. Y20210503). Natural Science Foundation of Liaoning Province (2022-NLTS-14-06).

Author Contributions: Y.L.: writing—original draft preparation. N.Y. and Z.W. : conceptualization, methodology, and funding acquisition. X.D. and J.L. : writing—review and editing and supervision. Y.D. and Y.W. : provided experimental method guidance, Y.Y and X.J. : data curation. Q.L. : generated and validated the mouse model.

Data Availability: The datasets generated during and/or analyzed during the current study are available from the corresponding author on reasonable request.

Ethics Approval Animal use has been approved by the Animal Use and Care Committee at Shenyang Medical College (protocol number: SYYXY2021031502).

Consent for Publication All authors have read and agreed to the published version of the manuscript.

Conflicts of Interest: The authors declare no conflicts of interest.

References

1. Zheng D, Liu Y, Luo L, Shahid MZ, Hou D (2020) Spatial variation and health risk assessment of fluoride in drinking water in the Chongqing urban areas, China. *Environmental geochemistry and health* 42:2925-2941. <https://doi.org/10.1007/s10653-020-00532-3>
2. Dall Agnol MA, Battiston C, Tenuta LMA, Cury JA (2022) Fluoride Formed on Enamel by Fluoride Varnish or Gel Application: A Randomized Controlled Clinical Trial. *Caries research* 56:73-80. <https://doi.org/10.1159/000521454>
3. Li X, Yang J, Liang C, Yang W, Zhu Q, Luo H, Liu X, Wang J, Zhang J (2022) Potential Protective Effect of Riboflavin Against Pathological Changes in the Main Organs of Male Mice Induced by Fluoride Exposure. *Biological trace element research* 200:1262-1273. <https://doi.org/10.1007/s12011-021-02746-7>
4. Lopes GO, Martins Ferreira MK, Davis L, Bittencourt LO, Bragança Aragão WA, Dionizio A, Rabelo Buzalaf MA, Crespo-Lopez ME, Maia CSF, Lima RR (2020) Effects of Fluoride Long-Term Exposure over the Cerebellum: Global Proteomic Profile, Oxidative Biochemistry, Cell Density, and Motor Behavior Evaluation. *International journal of molecular sciences* 21. <https://doi.org/10.3390/ijms21197297>
5. Łukomska A, Baranowska-Bosiacka I, Dec K, Pilutin A, Tarnowski M, Jakubczyk K, Żwieretło W, Skórka-Majewicz M, Chlubek D, Gutowska I (2020) Changes in Gene and Protein Expression of Metalloproteinase-2 and -9 and Their Inhibitors TIMP2 and TIMP3 in Different Parts of Fluoride-Exposed Rat Brain. *International journal of molecular sciences* 22. <https://doi.org/10.3390/ijms22010391>
6. Saeed M, Malik RN, Kamal A (2020) Fluorosis and cognitive development among children (6-14 years of age) in the endemic areas of the world: a review and critical analysis. *Environmental science and pollution research international* 27:2566-2579. <https://doi.org/10.1007/s11356-019-06938-6>
7. Ran LY, Xiang J, Zeng XX, Tang JL, Dong YT, Zhang F, Yu WF, Qi XL, Xiao Y, Zou J, Deng J, Guan ZZ (2021) Integrated transcriptomic and proteomic analysis indicated that neurotoxicity of rats with chronic fluorosis may be in mechanism involved in the changed cholinergic pathway and oxidative stress. *Journal of trace elements in medicine and biology : organ of the Society for Minerals and Trace Elements (GMS)* 64:126688. <https://doi.org/10.1016/j.jtemb.2020.126688>
8. Nadei OV, Khvorova IA, Agalakova NI (2020) Cognitive Decline of Rats with Chronic Fluorosis Is Associated with Alterations in Hippocampal Calpain Signaling. *Biological trace element research* 197:495-506. <https://doi.org/10.1007/s12011-019-01993-z>
9. Jiang P, Li G, Zhou X, Wang C, Qiao Y, Liao D, Shi D (2019) Chronic fluoride exposure induces neuronal apoptosis and impairs neurogenesis and synaptic plasticity: Role of GSK-3 β / β -catenin pathway. *Chemosphere* 214:430-435. <https://doi.org/10.1016/j.chemosphere.2018.09.095>
10. Beard E, Lengacher S, Dias S, Magistretti PJ, Finsterwald C (2021) Astrocytes as Key Regulators of Brain Energy Metabolism: New Therapeutic Perspectives. *Frontiers in physiology* 12:825816. <https://doi.org/10.3389/fphys.2021.825816>

11. Yamagata K (2022) Lactate Supply from Astrocytes to Neurons and its Role in Ischemic Stroke-induced Neurodegeneration. *Neuroscience* 481:219-231. <https://doi.org/10.1016/j.neuroscience.2021.11.035>
12. Pan SM, Pan Y, Tang YL, Zuo N, Zhang YX, Jia KK, Kong LD (2022) Thioredoxin interacting protein drives astrocytic glucose hypometabolism in corticosterone-induced depressive state. *Journal of neurochemistry* 161:84-100. <https://doi.org/10.1111/jnc.15489>
13. Schurr A, Passarella S (2022) Aerobic Glycolysis: A DeOxymoron of (Neuro)Biology. *Metabolites* 12. <https://doi.org/10.3390/metabo12010072>
14. Zheng J, Xie Y, Ren L, Qi L, Wu L, Pan X, Zhou J, Chen Z, Liu L (2021) GLP-1 improves the supportive ability of astrocytes to neurons by promoting aerobic glycolysis in Alzheimer's disease. *Molecular metabolism* 47:101180. <https://doi.org/10.1016/j.molmet.2021.101180>
15. Cunnane SC, Trushina E, Morland C, Prigione A, Casadesus G, Andrews ZB, Beal MF, Bergersen LH, Brinton RD, De La Monte S, Eckert A, Harvey J, Jeggo R, Jhamandas JH, Kann O, La Cour CM, Martin WF, Mithieux G, Moreira PI, Murphy MP, Nave KA, Nuriel T, Oliet SHR, Saudou F, Mattson MP, Swerdlow RH, Millan MJ (2020) Brain energy rescue: an emerging therapeutic concept for neurodegenerative disorders of ageing. *Nature reviews. Drug discovery* 19:609-633. <https://doi.org/10.1038/s41573-020-0072-x>
16. Xing G, Ren M, Watson WD, O'Neill JT, Verma A (2009) Traumatic brain injury-induced expression and phosphorylation of pyruvate dehydrogenase: a mechanism of dysregulated glucose metabolism. *Neuroscience letters* 454:38-42. <https://doi.org/10.1016/j.neulet.2009.01.047>
17. Lazzarino G, Amorini AM, Signoretti S, Musumeci G, Lazzarino G, Caruso G, Pastore FS, Di Pietro V, Tavazzi B, Belli A (2019) Pyruvate Dehydrogenase and Tricarboxylic Acid Cycle Enzymes Are Sensitive Targets of Traumatic Brain Injury Induced Metabolic Derangement. *International journal of molecular sciences* 20. <https://doi.org/10.3390/ijms20225774>
18. Solano Fonseca R, Metang P, Egge N, Liu Y, Zuurbier KR, Sivaprakasam K, Shirazi S, Chuah A, Arneaud SL, Konopka G, Qian D, Douglas PM (2021) Glycolytic preconditioning in astrocytes mitigates trauma-induced neurodegeneration. *eLife* 10. <https://doi.org/10.7554/eLife.69438>
19. Wang C, Zheng D, Weng F, Jin Y, He L (2022) Sodium butyrate ameliorates the cognitive impairment of Alzheimer's disease by regulating the metabolism of astrocytes. *Psychopharmacology* 239:215-227. <https://doi.org/10.1007/s00213-021-06025-0>
20. Stilling RM, Van De Wouw M, Clarke G, Stanton C, Dinan TG, Cryan JF (2016) The neuropharmacology of butyrate: The bread and butter of the microbiota-gut-brain axis? *Neurochemistry international* 99:110-132. <https://doi.org/10.1016/j.neuint.2016.06.011>
21. Campos-Perez W, Martinez-Lopez E (2021) Effects of short chain fatty acids on metabolic and inflammatory processes in human health. *Biochimica et biophysica acta. Molecular and cell biology of lipids* 1866:158900. <https://doi.org/10.1016/j.bbalip.2021.158900>
22. Angoa-Pérez M, Kuhn DM (2021) Evidence for Modulation of Substance Use Disorders by the Gut Microbiome: Hidden in Plain Sight. *Pharmacological reviews* 73:571-596.

<https://doi.org/10.1124/pharmrev.120.000144>

23. Tran SM, Mohajeri MH (2021) The Role of Gut Bacterial Metabolites in Brain Development, Aging and Disease. *Nutrients* 13. <https://doi.org/10.3390/nu13030732>
24. Jaworska J, Zalewska T, Sypecka J, Ziemka-Nalecz M (2019) Effect of the HDAC Inhibitor, Sodium Butyrate, on Neurogenesis in a Rat Model of Neonatal Hypoxia-Ischemia: Potential Mechanism of Action. *Molecular neurobiology* 56:6341-6370. <https://doi.org/10.1007/s12035-019-1518-1>
25. Jiang Y, Li K, Li X, Xu L, Yang Z (2021) Sodium butyrate ameliorates the impairment of synaptic plasticity by inhibiting the neuroinflammation in 5XFAD mice. *Chemico-biological interactions* 341:109452. <https://doi.org/10.1016/j.cbi.2021.109452>
26. Wang H, Song W, Wu Q, Gao X, Li J, Tan C, Zhou H, Zhu J, He Y, Yin J (2021) Fecal Transplantation from db/db Mice Treated with Sodium Butyrate Attenuates Ischemic Stroke Injury. *Microbiology spectrum* 9:e0004221. <https://doi.org/10.1128/Spectrum.00042-21>
27. Nitulescu GM, Van De Venter M, Nitulescu G, Ungurianu A, Juzenas P, Peng Q, Olaru OT, Grădinaru D, Tsatsakis A, Tsoukalas D, Spandidos DA, Margina D (2018) The Akt pathway in oncology therapy and beyond (Review). *International journal of oncology* 53:2319-2331. <https://doi.org/10.3892/ijo.2018.4597>
28. Sun LT, Zhang LY, Shan FY, Shen MH, Ruan SM (2021) Jiedu Sangen decoction inhibits chemoresistance to 5-fluorouracil of colorectal cancer cells by suppressing glycolysis via PI3K/AKT/HIF-1 α signaling pathway. *Chinese journal of natural medicines* 19:143-152. [https://doi.org/10.1016/s1875-5364\(21\)60015-8](https://doi.org/10.1016/s1875-5364(21)60015-8)
29. Duan F, Mei C, Yang L, Zheng J, Lu H, Xia Y, Hsu S, Liang H, Hong L (2020) Vitamin K2 promotes PI3K/AKT/HIF-1 α -mediated glycolysis that leads to AMPK-dependent autophagic cell death in bladder cancer cells. *Scientific reports* 10:7714. <https://doi.org/10.1038/s41598-020-64880-x>
30. Wang P, Cong M, Liu T, Li Y, Liu L, Sun S, Sun L, Zhu Z, Ma H, You H, Zhang H, Jia J (2020) FoxA2 inhibits the proliferation of hepatic progenitor cells by reducing PI3K/Akt/HK2-mediated glycolysis. *Journal of cellular physiology* 235:9524-9537. <https://doi.org/10.1002/jcp.29759>
31. Niu R, Chen H, Manthari RK, Sun Z, Wang J, Zhang J, Wang J (2018) Effects of fluoride on synapse morphology and myelin damage in mouse hippocampus. *Chemosphere* 194:628-633. <https://doi.org/10.1016/j.chemosphere.2017.12.027>
32. Xin J, Zeng D, Wang H, Sun N, Khaliq A, Zhao Y, Wu L, Pan K, Jing B, Ni X (2020) *Lactobacillus johnsonii* BS15 improves intestinal environment against fluoride-induced memory impairment in mice—a study based on the gut-brain axis hypothesis. *PeerJ* 8:e10125. <https://doi.org/10.7717/peerj.10125>
33. Endemic fluorosis research institute of china endemic disease prevention and control research center (2001) Determination for fluoride in Serum - Ion selective electrode method. National public service platform for standards information. <https://std.samr.gov.cn/hb/search/stdHBDetailed?id=8B1827F1C221BB19E05397BE0A0AB44A>

34. Endemic fluorosis research institute of china endemic disease prevention and control research center (2015) Determination for fluoride in urine - Ion selective electrode method. National public service platform for standards information. <https://std.samr.gov.cn/hb/search/stdHBDetailed?id=8B1827F231E7BB19E05397BE0A0AB44A>
35. Qiao L, Liu X, He Y, Zhang J, Huang H, Bian W, Chilufya MM, Zhao Y, Han J (2021) Progress of Signaling Pathways, Stress Pathways and Epigenetics in the Pathogenesis of Skeletal Fluorosis. *International journal of molecular sciences* 22. <https://doi.org/10.3390/ijms222111932>
36. Guth S, Hüser S, Roth A, Degen G, Diel P, Edlund K, Eisenbrand G, Engel KH, Epe B, Grune T, Heinz V, Henle T, Humpf HU, Jäger H, Joost HG, Kulling SE, Lampen A, Mally A, Marchan R, Marko D, Mühle E, Nitsche MA, Röhrdanz E, Stadler R, Van Thriel C, Vieths S, Vogel RF, Wascher E, Watzl C, Nöthlings U, Hengstler JG (2020) Toxicity of fluoride: critical evaluation of evidence for human developmental neurotoxicity in epidemiological studies, animal experiments and in vitro analyses. *Archives of toxicology* 94:1375-1415. <https://doi.org/10.1007/s00204-020-02725-2>
37. Grandjean P (2019) Developmental fluoride neurotoxicity: an updated review. *Environmental health : a global access science source* 18:110. <https://doi.org/10.1186/s12940-019-0551-x>
38. Ning H, Li C, Yin Z, Hu D, Ge Y, Chen L (2021) Fluoride exposure decreased neurite formation on cerebral cortical neurons of SD rats in vitro. *Environmental science and pollution research international* 28:50975-50982. <https://doi.org/10.1007/s11356-021-13950-2>
39. Kitahara M, Inoue T, Mani H, Takamatsu Y, Ikegami R, Tohyama H, Maejima H (2021) Exercise and pharmacological inhibition of histone deacetylase improves cognitive function accompanied by an increase of gene expressions crucial for neuronal plasticity in the hippocampus. *Neuroscience letters* 749:135749. <https://doi.org/10.1016/j.neulet.2021.135749>
40. Sun J, Yuan B, Wu Y, Gong Y, Guo W, Fu S, Luan Y, Wang W (2020) Sodium Butyrate Protects N2a Cells against A β Toxicity In Vitro. *Mediators of inflammation* 2020:7605160. <https://doi.org/10.1155/2020/7605160>
41. Zeng XX, Deng J, Xiang J, Dong YT, Cao K, Liu XH, Chen D, Ran LY, Yang Y, Guan ZZ (2020) Protections against toxicity in the brains of rat with chronic fluorosis and primary neurons exposed to fluoride by resveratrol involves nicotinic acetylcholine receptors. *Journal of trace elements in medicine and biology : organ of the Society for Minerals and Trace Elements (GMS)* 60:126475. <https://doi.org/10.1016/j.jtemb.2020.126475>
42. Sacks D, Baxter B, Campbell BCV, Carpenter JS, Cognard C, Dippel D, Eesa M, Fischer U, Hausegger K, Hirsch JA, Shazam Hussain M, Jansen O, Jayaraman MV, Khalessi AA, Kluck BW, Lavine S, Meyers PM, Ramee S, Rüfenacht DA, Schirmer CM, Vorwerk D (2018) Multisociety Consensus Quality Improvement Revised Consensus Statement for Endovascular Therapy of Acute Ischemic Stroke. *International journal of stroke : official journal of the International Stroke Society* 13:612-632. <https://doi.org/10.1177/1747493018778713>
43. Fernando W, Martins IJ, Morici M, Bharadwaj P, Rainey-Smith SR, Lim WLF, Martins RN (2020) Sodium Butyrate Reduces Brain Amyloid- β Levels and Improves Cognitive Memory Performance in

- an Alzheimer's Disease Transgenic Mouse Model at an Early Disease Stage. *Journal of Alzheimer's disease* : JAD 74:91-99. <https://doi.org/10.3233/jad-190120>
44. Badejogbin C, Areola DE, Olaniyi KS, Adeyanju OA, Adeosun IO (2019) Sodium butyrate recovers high-fat diet-fed female Wistar rats from glucose dysmetabolism and uric acid-associated cardiac tissue damage. *Naunyn-Schmiedeberg's archives of pharmacology* 392:1411-1419. <https://doi.org/10.1007/s00210-019-01679-2>
45. Amoêdo ND, Rodrigues MF, Pezzuto P, Galina A, Da Costa RM, De Almeida FC, El-Bacha T, Rumjanek FD (2011) Energy metabolism in H460 lung cancer cells: effects of histone deacetylase inhibitors. *PloS one* 6:e22264. <https://doi.org/10.1371/journal.pone.0022264>
46. Zhou T, Xu H, Cheng X, He Y, Ren Q, Li D, Xie Y, Gao C, Zhang Y, Sun X, Xu Y, Huang W (2022) Sodium Butyrate Attenuates Diabetic Kidney Disease Partially via Histone Butyrylation Modification. *Mediators of inflammation* 2022:7643322. <https://doi.org/10.1155/2022/7643322>
47. Yellen G (2018) Fueling thought: Management of glycolysis and oxidative phosphorylation in neuronal metabolism. *The Journal of cell biology* 217:2235-2246. <https://doi.org/10.1083/jcb.201803152>
48. Bell SM, Burgess T, Lee J, Blackburn DJ, Allen SP, Mortiboys H (2020) Peripheral Glycolysis in Neurodegenerative Diseases. *International journal of molecular sciences* 21. <https://doi.org/10.3390/ijms21238924>
49. Alberini CM, Cruz E, Descalzi G, Bessières B, Gao V (2018) Astrocyte glycogen and lactate: New insights into learning and memory mechanisms. *Glia* 66:1244-1262. <https://doi.org/10.1002/glia.23250>
50. Gray LR, Tompkins SC, Taylor EB (2014) Regulation of pyruvate metabolism and human disease. *Cellular and molecular life sciences* : CMLS 71:2577-2604. <https://doi.org/10.1007/s00018-013-1539-2>
51. Harris RA, Tindale L, Lone A, Singh O, Macauley SL, Stanley M, Holtzman DM, Bartha R, Cumming RC (2016) Aerobic Glycolysis in the Frontal Cortex Correlates with Memory Performance in Wild-Type Mice But Not the APP/PS1 Mouse Model of Cerebral Amyloidosis. *The Journal of neuroscience : the official journal of the Society for Neuroscience* 36:1871-1878. <https://doi.org/10.1523/jneurosci.3131-15.2016>
52. Yang SQ, Tian Q, Li D, He SQ, Hu M, Liu SY, Zou W, Chen YJ, Zhang P, Tang XQ (2020) Leptin mediates protection of hydrogen sulfide against 6-hydroxydopamine-induced Parkinson's disease: Involving enhancement in Warburg effect. *Neurochemistry international* 135:104692. <https://doi.org/10.1016/j.neuint.2020.104692>
53. Chin YR, Toker A (2009) Function of Akt/PKB signaling to cell motility, invasion and the tumor stroma in cancer. *Cellular signalling* 21:470-476. <https://doi.org/10.1016/j.cellsig.2008.11.015>
54. Robey RB, Hay N (2009) Is Akt the "Warburg kinase"?-Akt-energy metabolism interactions and oncogenesis. *Seminars in cancer biology* 19:25-31. <https://doi.org/10.1016/j.semcancer.2008.11.010>

55. Kim JW, Tchernyshyov I, Semenza GL, Dang CV (2006) HIF-1-mediated expression of pyruvate dehydrogenase kinase: a metabolic switch required for cellular adaptation to hypoxia. *Cell metabolism* 3:177-185. <https://doi.org/10.1016/j.cmet.2006.02.002>
56. Marín-Hernández A, Gallardo-Pérez JC, Ralph SJ, Rodríguez-Enríquez S, Moreno-Sánchez R (2009) HIF-1alpha modulates energy metabolism in cancer cells by inducing over-expression of specific glycolytic isoforms. *Mini reviews in medicinal chemistry* 9:1084-1101. <https://doi.org/10.2174/138955709788922610>
57. Sun R, Meng X, Pu Y, Sun F, Man Z, Zhang J, Yin L, Pu Y (2019) Overexpression of HIF-1a could partially protect K562 cells from 1,4-benzoquinone induced toxicity by inhibiting ROS, apoptosis and enhancing glycolysis. *Toxicology in vitro : an international journal published in association with BIBRA* 55:18-23. <https://doi.org/10.1016/j.tiv.2018.11.005>
58. Zhou Z, Xu N, Matei N, McBride DW, Ding Y, Liang H, Tang J, Zhang JH (2021) Sodium butyrate attenuated neuronal apoptosis via GPR41/Gβγ/PI3K/Akt pathway after MCAO in rats. *Journal of cerebral blood flow and metabolism : official journal of the International Society of Cerebral Blood Flow and Metabolism* 41:267-281. <https://doi.org/10.1177/0271678x20910533>

Tables

Table 1 Body weight, brain weight, and fluorine content in blood and urine of mice.

Experimental group	Body weight (g)	Brain weight (g)	Fluoride content in serum (mg/L)	Fluoride content in urine (mg/L)
C	48.58±0.749	0.4218±0.006	0.1790±0.005	1.131±0.167
SB	45.70±1.009	0.4199±0.008	0.1771±0.003	1.069±0.172
F	40.20±1.652**	0.3915±0.006*	0.2185±0.008**	8.908±0.316**
F+SB1	43.69±1.494	0.3970±0.007#	0.2055±0.005**	8.599±0.440**
F+SB2	45.10±0.8781#	0.4263±0.009#	0.1905±0.010**	8.023±0.430**

All values are expressed as the mean ± SEM ($n = 10$). * $p < 0.05$, ** $p < 0.01$ vs. C mice, # $p < 0.05$, ## $p < 0.01$ vs. F mice.

Figures

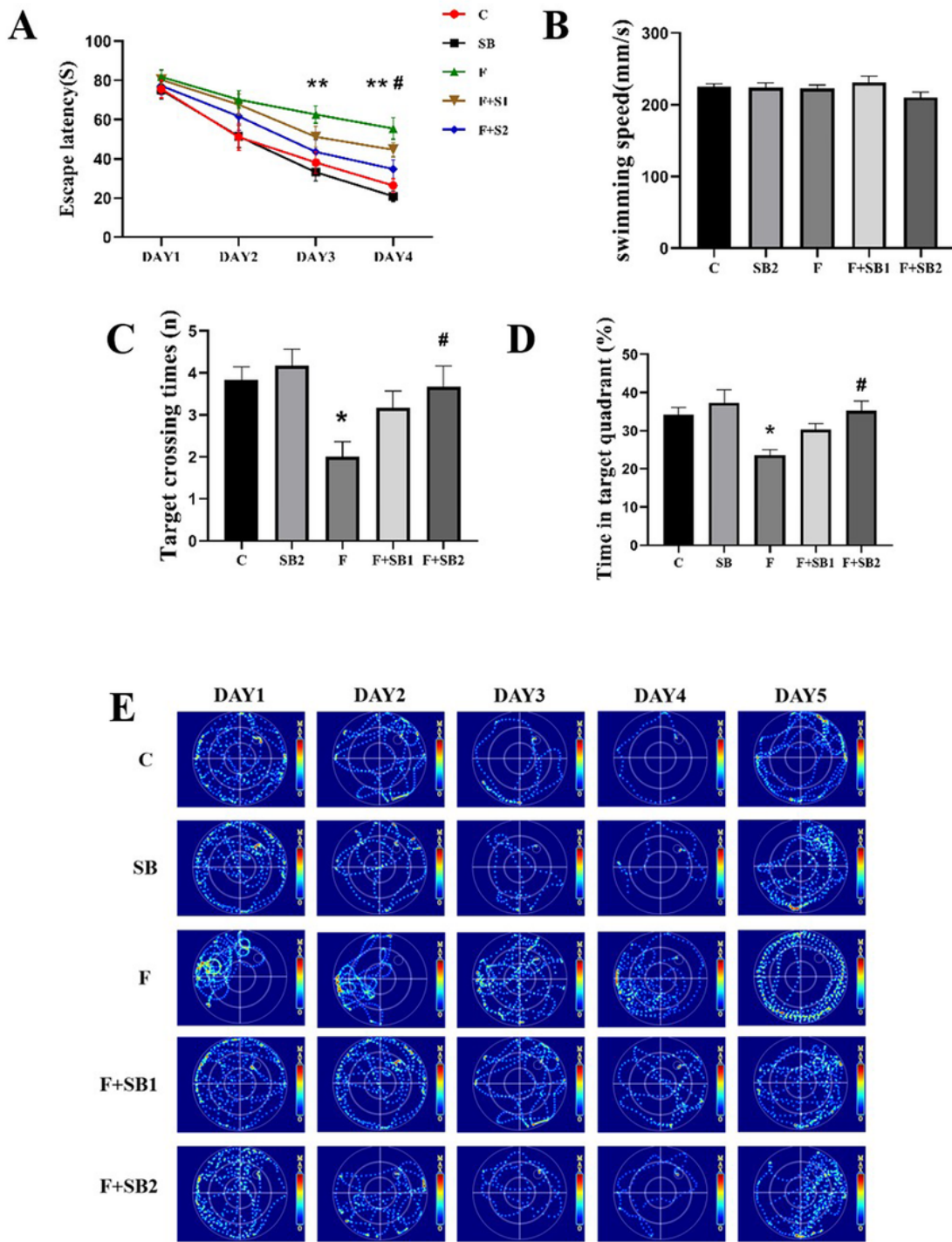


Figure 1

After 8 weeks of sodium butyrate treatment, mice in each group were subjected to Morris water maze to observe the changes of spatial learning and memory. 1000mg/kg sodium butyrate improves spatial learning and memory in fluorosis-treated rats. (A) escape incubation period, (B) swimming speed, (C) number of times the escape platform was crossed, (D) the percentage of swimming time in the target

quadrant, and (E) representative swimming tracks. All values are expressed as the mean \pm SEM ($n = 6$).
* $p < 0.05$ vs. C mice, # $p < 0.05$ vs. F mice.

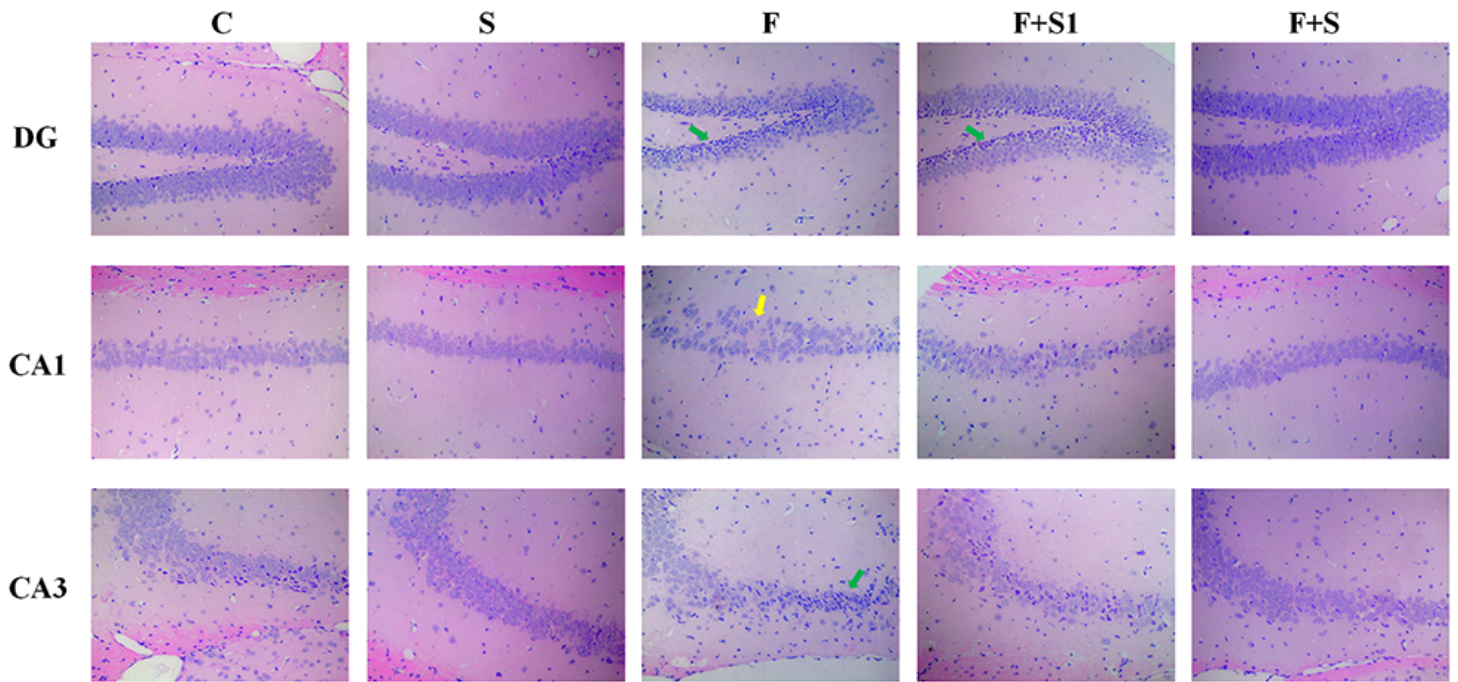


Figure 2

The results of HE staining showed that sodium butyrate ameliorated the damage of hippocampus in fluorosis mice, $\times 300$. (DG: dentate gyrus, CA1: hippocampal CA1 region, CA2: hippocampal CA2 region, the green arrow indicates cell shrinkage and the yellow arrow indicates cell gap enlargement and loose arrangement $n=3$)

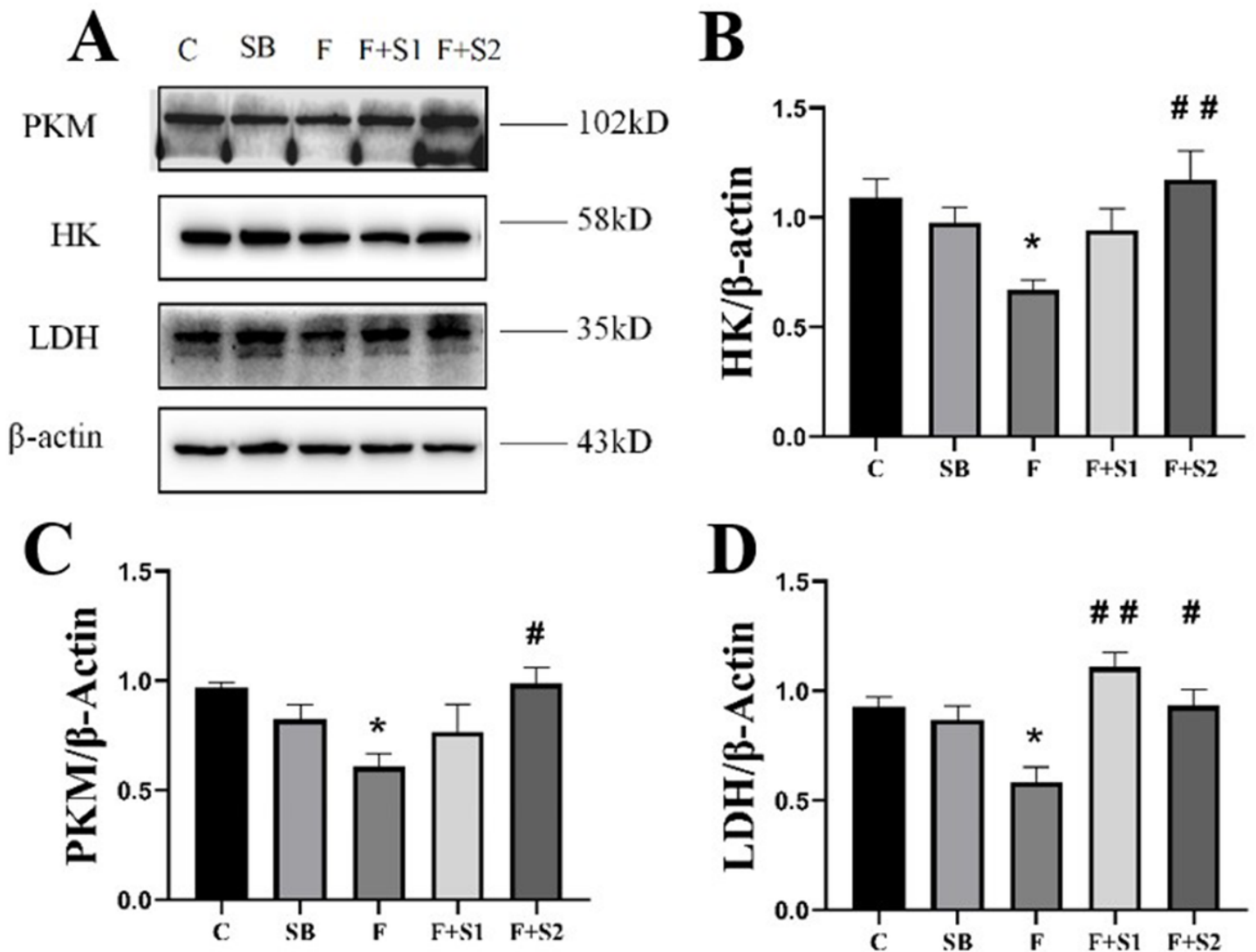


Figure 3

Effects of sodium butyrate and fluorosis on glycolysis key enzymes (HK, PKM and LDH) in hippocampus by western blot. The expression of PKM, LDH, and HK in hippocampus (A) and the quantitative analysis of optical density(B-D). All values were expressed as the mean \pm SEM (n = 4). *p < 0.05 vs. C mice, #p < 0.05, ##p < 0.01 vs. F mice.

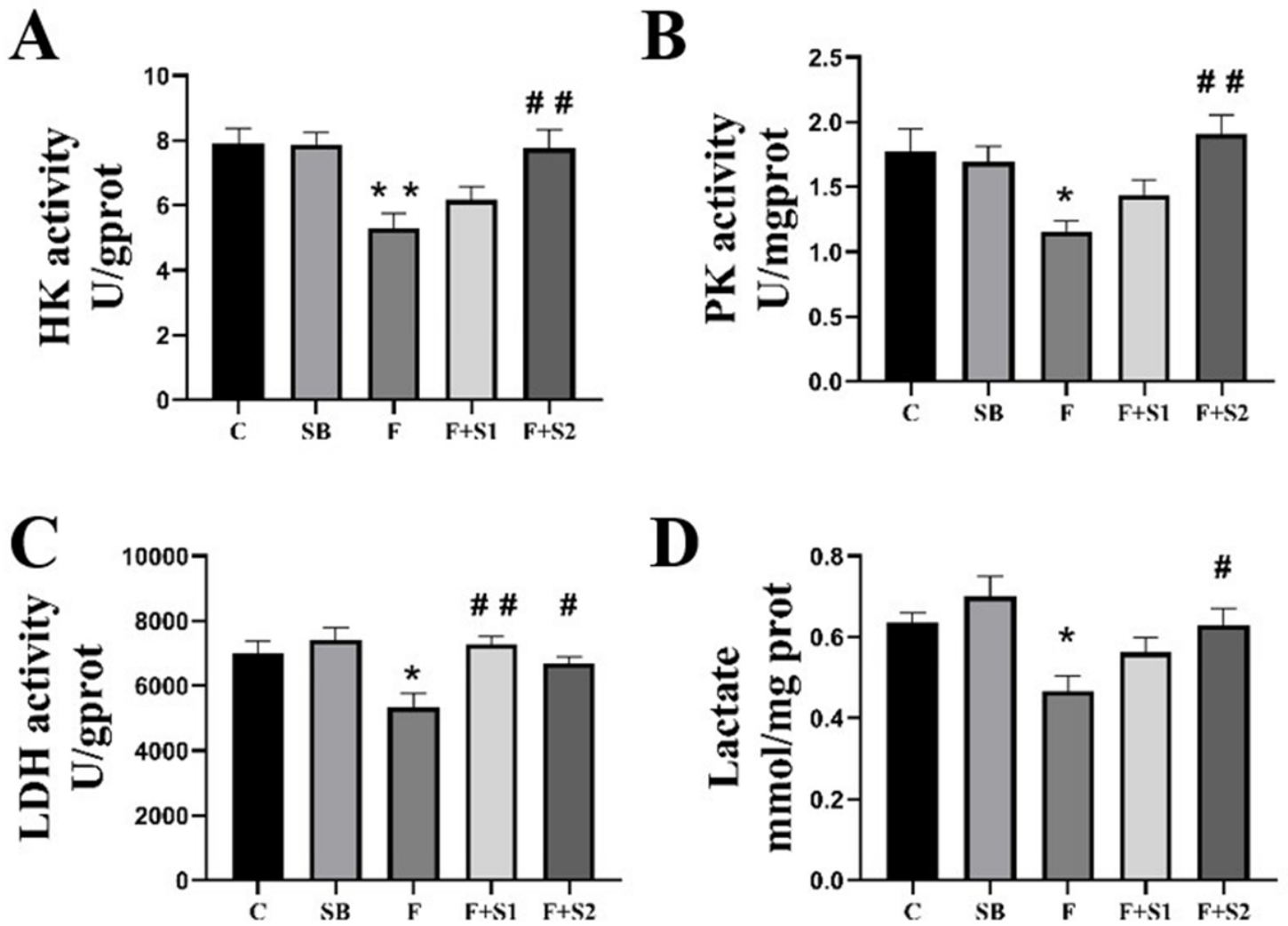


Figure 4

Effects of sodium butyrate and fluorosis on glycolysis key enzymes (HK, PKM and LDH) in hippocampus by Assay Kit. The activity of HK (A), PK (B), and LDH (C) and content of lactate (D) in hippocampus. All values were expressed as the mean \pm SEM ($n = 6$). * $p < 0.05$, ** $p < 0.01$ vs. C mice, # $p < 0.05$, ## $p < 0.01$ vs. F mice.

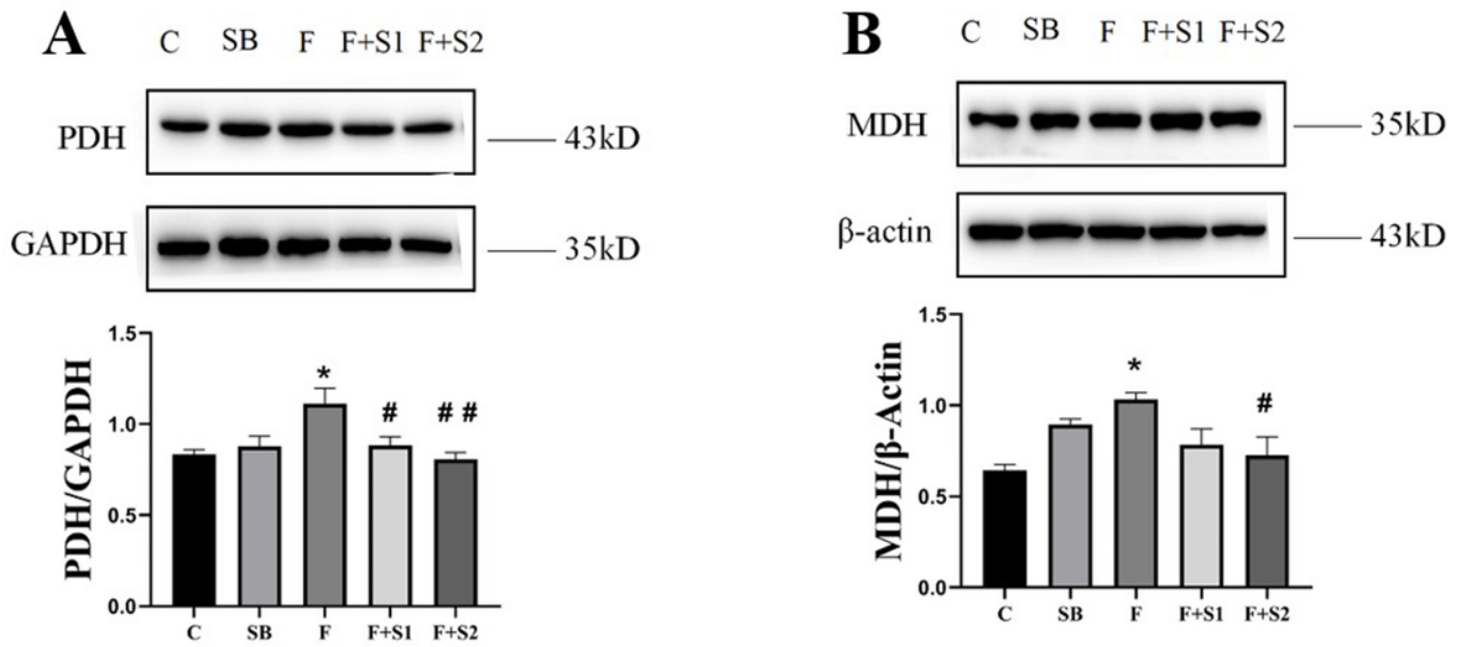


Figure 5

Effects of sodium butyrate and fluorosis on pyruvate metabolism in hippocampus by western blot. The expression of PDH (A) and MDH (B) in hippocampus and the quantitative analysis of optical density. All values were expressed as the mean \pm SEM ($n = 4$). * $p < 0.05$ vs. C mice, # $p < 0.05$, ## $p < 0.01$ vs. F mice.

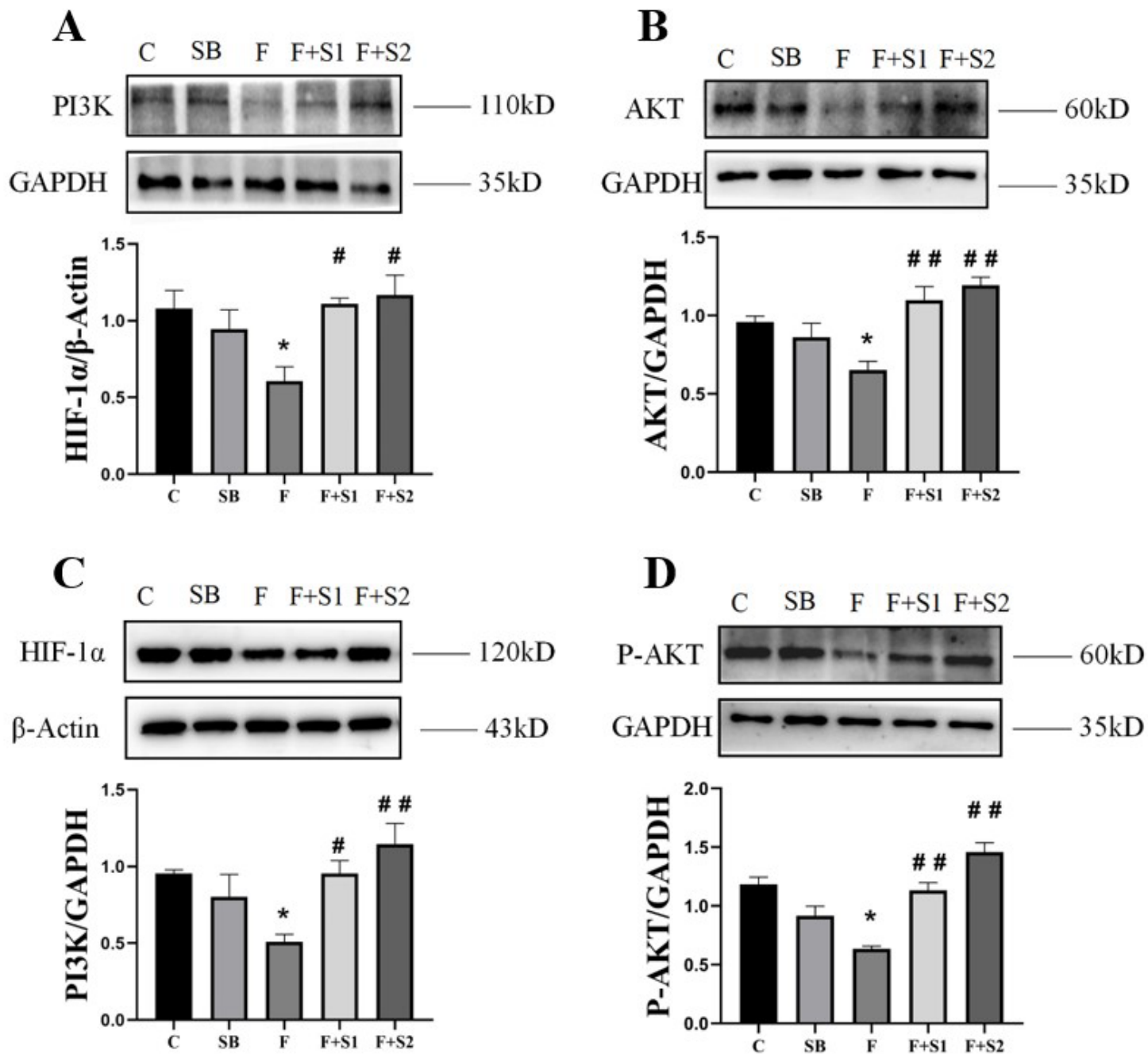


Figure 6

Effects of sodium butyrate and fluorosis on PI3K/AKT/HIF-1 α pathway in hippocampus by western blot. The expression of PI3K (A), AKT (B), P-AKT (C) and HIF-1 α (D) in hippocampus and the quantitative analysis of optical density. All values were expressed as the mean \pm SEM (n = 4). *p < 0.05 vs. C mice, #p < 0.05, ##p < 0.01 vs. F mice.